RZ 3390 (# 93436) 01/14/02
Mathematics & Physics 6 pages

Research Report

Comparison of the Emission Spectra of Organic Lasers with Calculated Dispersion Relations

N. Moll,[1] C. Bauer,[2] B. Schnabel,[3] E. B. Kley,[4] U. Scherf,[5] and R. F. Mahrt[1]

[1]IBM Research, Zurich Research Laboratory
8803 Rüschlikon, Switzerland

[2]Philipps-Universität Marburg, Fachbereich Physik
35032 Marburg, Germany

[3]Leica Microsystems Lithography GmbH
07745 Jena, Germany

[4]Friedrich-Schiller Universität Jena, Institut für Angewandte Physik
07743 Jena, Germany

[5]Universität Potsdam, Institut für Physikalische und Theoretische Chemie
14476 Golm, Germany

LIMITED DISTRIBUTION NOTICE

This report has been submitted for publication outside of IBM and will probably be copyrighted if accepted for publication. It has been issued as a Research Report for early dissemination of its contents. In view of the transfer of copyright to the outside publisher, its distribution outside of IBM prior to publication should be limited to peer communications and specific requests. After outside publication, requests should be filled only by reprints or legally obtained copies of the article (e.g., payment of royalties). Some reports are available at http://domino.watson.ibm.com/library/Cyberdig.nsf/home.

Research
Almaden · Austin · Beijing · Delhi · Haifa · T.J. Watson · Tokyo · Zurich

Comparison of the Emission Spectra of Organic Lasers with Calculated Dispersion Relations

N. Moll,[1] C. Bauer,[2] B. Schnabel,[3] E. B. Kley,[4] U. Scherf,[5] and R. F. Mahrt[1]

[1] *IBM Research, Zurich Research Laboratory, CH-8803 Rüschlikon, Switzerland*

[2] *Philipps-Universität Marburg, Fachbereich Physik, Renthof 5, D-35032 Marburg, Germany*

[3] *Leica Microsystems Lithography GmbH, Göschwitzer Str. 25, D-07745 Jena, Germany*

[4] *Friedrich-Schiller Universität Jena, Institut für Angewandte Physik, Max-Wien Platz 1, D-07743 Jena, Germany*

[5] *Universität Potsdam, Institut für Physikalische und Theoretische Chemie, Karl-Liebknecht-Str. 24-25, D-14476 Golm, Germany*

Abstract

The emission spectra of optically pumped organic semiconductor lasers are compared with calculated dispersion relations of the dielectric feedback systems of the lasers. The lasers are fabricated by spin coating a thin film of a methyl-substituted ladder-type poly-(para-phenylene) onto a nano-patterned circular-grating distributed Bragg reflector. The lasing is located spectrally at the band edge of the Bragg dip, and can be tuned by varying the period of the grating.

Owing to their high optical gain, their spectrally broad gain region, and their low production costs, organic semiconductors have great potential for photonic applications. Solution-deposited conjugated polymers as well as evaporated small molecules have been used as gain materials in various geometries of organic semiconductor lasers.[1–5] An optimum photon confinement is crucial to obtain a substantial decrease in the lasing threshold.[6] This optimum confinement can be achieved by exploiting three-dimensional photonic band gap (PBG) structures. However, it is very difficult to fabricate a high-quality three-dimensional structure in the visible spectral range. We therefore fabricated a circular-grating surface-emitting distributed Bragg resonator that provides an almost complete two-dimensional feedback.[7–9]

Figure 1 shows a schematic cross section of the distributed feedback structure under investigation. The active material consists of a methyl-substituted ladder-type poly(paraphenylene) (MeLPPP) that has both excellent opto-electronic properties and a high optical gain of about 2000 cm^{-1}.[10] The circular-grating structures were fabricated from fused silica substrates by using electron-beam lithography and ion-beam etching. Four different grating periods Λ were chosen, namely 298, 305, 318, and 325 nm. As will be shown later, grating periods in that range match the second-order Bragg condition for the wavelength of the organic material. Two different duty cycles (ratio between ridge and groove) were studied with a ratio of 1 to 1.22 and 1 to 4. The diameter of the inner ring was 9 Λ, the depth of the grooves was about 150 nm, and the overall diameter of the circular grating 100 μm. The film thickness of the MeLPPP was measured to be approx. 290 nm. Further details of the experimental configuration are given in Ref. 11.

The grating-polymer structures were uniformly illuminated by 20 ns pulses of an excimer pumped dye-laser system at a photon energy of 2.78 eV. The emitted light was collected by an optical multichannel analyzer equipped with a liquid-nitrogen-cooled CCD camera with an overall spectral resolution of about 1 meV. All measurements were performed at room temperature and in a vacuum at low pressure (10^{-4} mbar) to prevent photo-oxidation processes. Above a certain pump threshold, all structures—independent of grating period and duty cycle—exhibit clear laser action, in contrast to previous studies with thinner films of about 130-nm film thickness.[11] This is due to a larger quantity of gain material and higher-order modes in the devices fabricated with the thicker film. This will be discussed more in detail later in the paper.

To obtain deeper insight into the lasing action, we first theoretically investigate a simplified configuration instead of the full grating configuration. The radial or more or less quasi-radial modes of the circular grating should correspond to eigenmodes of the linear grating.[8] Furthermore, the actual photon confinement is solely due to the grooves. Therefore, we calculate the dispersion relations of multilayer films for the two duty cycles. The multilayers consist of alternating organic and quartz layers. The duty cycles are varied by changing the layer thickness of the organic and quartz films. The dispersion relations are given by the eigenmodes which are obtained by numerically solving Maxwell's equations in the frequency domain[12] of the dielectric system for different wavevectors. For these one-dimensional multilayer films, the modes are expanded into plane waves. The structures are repeated periodically within the supercell approximation. The supercell has a size of 1 a, where a is the lattice constant and equal to the grating period Λ. Convergence tests show that 32 plane waves suffice to resolve the frequencies of dielectric structures for the supercell. A conjugate gradient minimization is applied to obtain the eigenmodes. The eigenvalues are

considered converged when the fractual change of the eigenvalues is smaller than 10^{-4}.

In Fig. 2 the dispersion relations of multilayer films are shown. Because of symmetry both polarizations, transverse electric (TE) and transverse magnetic (TM), are degenerate and result in the same dispersion relations. For both duty cycles small band gaps are formed at the edges of the Brillouin zone, e.g., for the wavevectors $k = 0$ and $k = 0.52\pi/a$. Owing to the band gaps, the group velocity becomes zero at the Brillouin zone edges. At these wavevectors, the density of photonic states is increased. Standing waves are formed, which provide the ample feedback necessary for the laser action. In our case the second-order band gap, i.e., the Bragg condition, at a wavevector of $k = 0$ is the interesting one. Its frequency range of 0.63 to 0.68 c/a corresponds to 438 to 500 nm for grating periods between 298 and 325 nm. This is exactly the frequency range in which the optical gain for the MeLPPP material is the highest. Figure 2 clearly reveals that for a duty cycle of 1 to 4 the second-order band gap is considerably larger than for a duty cycle of 1 to 1.22. More states have to be redistributed out of the region where the band gap lies, and the bands will have a stronger band bending near the wavevector $k = 0$. Therefore, a larger number of wavevectors have a group velocity close to zero. Hence in this case one expects a larger increase of the density of states at the band-gap edges and better photon confinement. This is experimentally confirmed by the about three times smaller lasing threshold for the grating with a duty cycle of 1 to 4.

As a next step, we calculate the eigenmodes of the corresponding linear grating, which has the same cross section as the circular grating. Now additionally the finite height of the grooves and the film of organic material above them are taken into account. This system is two-dimensional, and the supercell has to be enlarged perpendicular to the grating. A supercell of 16 a by 1 a is used, leading to 16,384 plane waves, i.e., using 32 plane waves per grating period. Convergence tests show that this number of plane waves is sufficient to resolve the eigenmodes. We calculate the eigenmodes of this linear grating for the two different duty cycles and the four different grating periods. In Fig. 3 the results for a grating period of 298 nm are shown. Only those eigenmodes are shown in which the major part of the energy is located within the organic material. Beside these eigenmodes, there are also many unbound modes or resonances due to the vacuum and substrate. In contrast to the multilayer-film configuration, here the two polarizations TE and TM are not degenerate. For both polarizations the lower and upper band of the eigenmodes are separated by a small band gap. The symmetries of the two bands differ. In the groove region, the lower band has a maximum and the upper band a minimum for the intensity of the electric displacement field. Comparing the thicker film of 290 nm with the thinner film of 130 nm[11] reveals that also higher-order bands appear. These bands are due to the fact that now the organic film has a sufficient thickness to support higher-order modes, which have a nodal plane in the organic film. This can be seen from the intensity distribution of the electric displacement fields for TE polarization. For TM polarization, the higher-order upper band coincides with many unbound eigenmodes of the vacuum and cannot be resolved computationally.

In Fig. 4 the combined experimental and computational results are shown for the two duty cycles. In contrast to the thinner film of 130 nm,[11] three Bragg dips are observed experimentally for each grating period. As expected from the Bragg condition, their wavelengths increase linearly with the grating period. For each grating period one lasing peak is observed. For the smaller grating periods of 298 and 305 nm, the lasing occurs at the

band edges of the Bragg dip with the largest wavelength. For the larger grating periods of 318 and 325 nm, the lasing occurs at other Bragg dips, namely at those having the second largest wavelength. The lasing always occurs at the Bragg dips that are closer to the gain maximum of the material, which is around 492 nm. However, this argument provides no information on which side of the Bragg dip the lasing action will occur. For example, for the sample with a duty cycle of 1 to 1.22 and a grating period of 325 nm, the lasing does not occur at the higher wavelength of the Bragg dip, as would be expected, but at the lower. Imperfections of the samples are probably a reason for the preference of one lasing mode over the other.

It is not easy to relate the experimental measurements to the computed band gaps. A further difficulty arises because of the circular symmetry of the system, which makes it impossible to determine experimentally which polarization is emitted. The computed band gaps lie in the same wavelength range as the experimental ones, and also increase linearly with the grating period. A decrease in the duty cycle leads to an increase of the band-gap widths. Computationally four band gaps are found whereas experimentally only three are observed. This suggests that the experimental Bragg dip with the largest wavelength corresponds to the higher TE band gap, and that the experimental Bragg dip with the second largest wavelength corresponds to the higher TM band gap. The Bragg dip with the smallest wavelength then either corresponds to the lower TE or TM band gap of the higher-order modes. Assuming that this classification is correct, the question remains why the experimentally observed TE and TM Bragg dips lie further apart than the computed eigenmodes. This can easily be explained by the uncertainty in the film thickness, which is the parameter with a large measurement error. A thinner film gives rise to a larger difference in the TE and TM modes, as was shown in Ref. 11. Indeed, a film thickness of 200 nm will give a difference in the TE and TM modes of about 14 nm, which is comparable to the experimentally observed one of about 16 nm. Other errors, such as the measured duty cycles and grating periods, could lead to larger differences between the experimental the and computed lasing wavelength. An uncertainty of 5% in the grating period directly leads to a 5% uncertainty in the Bragg wavelength, which corresponds to approx. 25 nm, i.e. about the difference between experiment and theory. Considering all the uncertainties in the fabrication of these structures, the agreement between experimental and computational results is quite astonishing.

In conclusion, we have compared the spectrum of an optically pumped organic laser having two-dimensional confinement with computed dispersion relations. The lasing wavelength can be tuned by varying the grating period of the confining structure. The two-dimensional confinement of the circular grating redistributes the density of states, and increases it at the band edges. This increase then gives rise to the lasing action.

We gratefully acknowledge support by the Volkswagen-Stiftung and Fonds der Chemischen Industrie.

[1] J. H. Burroughes, D. D. C. Bradley, A. R. Brown, R. N. Marks, K. Mackay, R. H. Friend, P. L. Burns, A. B. Burns, and A. B. Holmes, Science **347**, 539 (1990)
[2] N. Tessler, G. J. Denton, and R. H. Friend, Nature **382**, 695 (1996).
[3] C. Kallinger, M. Hilmer, A. Haugeneder, M. Perner, W. Spirkel, U. Lemmer, J. Feldmann, U. Scherf, K. Mllen, A. Gombert, and V. Wittwer, Adv. Mater. **10**, 920 (1998).
[4] G. Wegmann, H. Giessen, D. Hertel, and R. F. Mahrt, Solid State Commun. **37**, 510 (1997).
[5] S. V. Frolov, Z. V. Vardeny, and K. Yoshino, Appl. Phys. Lett. **72**, 2811 (1998).
[6] M. Meier, A. Mekis, A. Dodabalapur, A. Timko, R. E. Slusher, J. D. Joannopoulos, and O. Nalamasu, Appl. Phys. Lett. **74**, 7 (1999).
[7] T. Erdogan, O. King, G. W. Wicks, D. G. Hall, E. H. Anderson, and M. J. Rooks, Appl. Phys. Lett. **60**, 1921 (1992).
[8] D. Labilloy, H. Benisty, C. Weisbuch, T. F. Krauss, C. J. M. Smith, R. Houdre, and U. Oesterle, Appl. Phys. Lett. **73**, 1314 (1998).
[9] C. Bauer, H. Giessen, B. Schnabel, E. B. Kley, C. Schmitt, U. Scherf, and R. F. Mahrt, Adv. Mater. **13**, 1161 (2001).
[10] G. Wegmann, B. Schweitzer, D. Hertel, M. Oestreich, U. Scherf, K. Mllen, and R. F. Mahrt, Chem. Phys. Lett. **312**, 376 (1999).
[11] N. Moll, C. Bauer, H. Giessen, B. Schnabel, E. B. Kley, U. Scherf, and R. F. Mahrt, accepted for publication in Appl. Phys. Lett. (2001).
[12] S. G. Johnson and J. D. Joannopoulos, Optics Express **8**, 173 (2001).

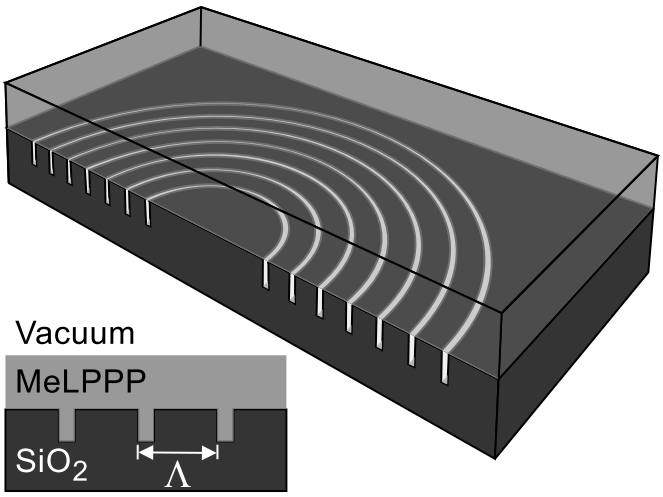

FIG. 1. Schematic cross section of the circular grating in the quartz substrate with the MeLPPP film with a duty cycle of 1 to 4.

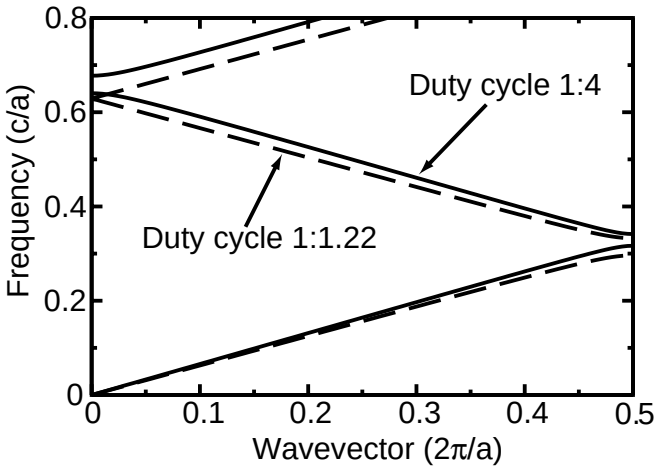

FIG. 2. Dispersion relations of a multilayer structure consisting of quartz and MeLPPP for the duty cycles 1 to 4 (solid) and 1 to 1.22 (dashed).

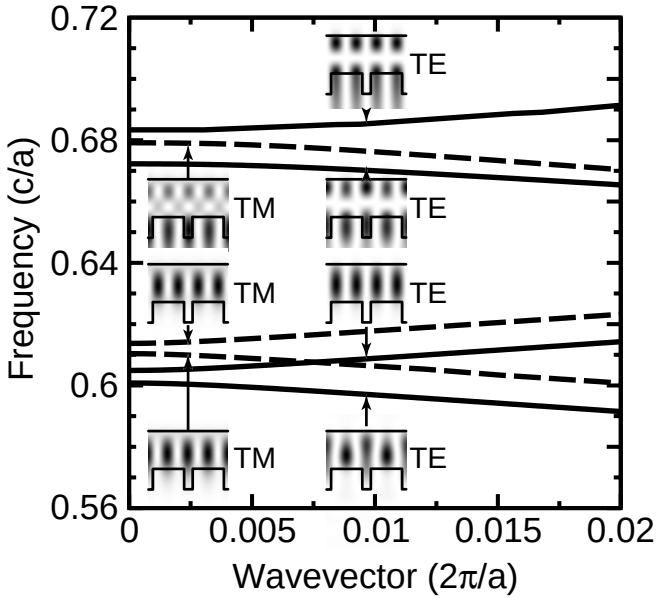

FIG. 3. The calculated dispersion relations for a linear grating with a period of 298 nm and a duty cycle of 1 to 4. The frequency of the TE and the TM mode is plotted versus the wavevector as solid and dashed line, respectively. The units are normalized by the lattice constant a. The intensities of the electric displacement field for the TE and TM modes are plotted for a wavevector equal to zero.

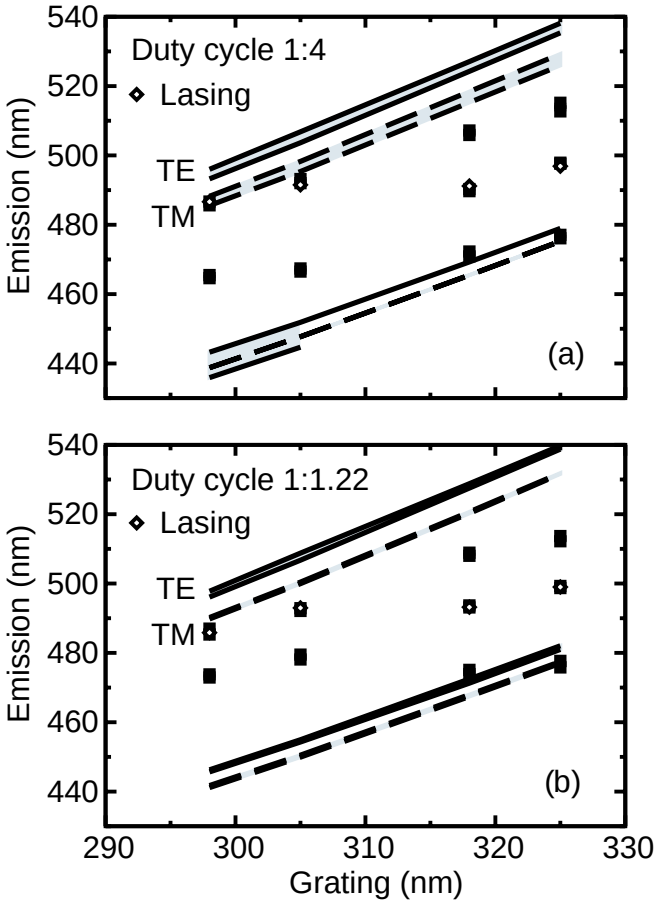

FIG. 4. Comparison of measured and calculated frequencies for the two duty cycles and the four grating periods. (a) displays the results for a duty cycle of 1 to 4, and (b) for a duty cycle of 1 to 1.22. The diamonds correspond to the measured lasing frequencies plotted for the four different grating periods. The frequency range of the Bragg dips is indicated by the black rectangles. The calculated TE and TM band edges are plotted as solid and dashed lines, respectively. The band gaps correspond to the shaded areas. For the grating periods of 318 and 325 nm, the lower band of the higher-order TE mode coincides with many resonances and cannot be resolved computationally.